IET Energy Systems Integration

Research Article

IET Journals
The Institution of Engineering and Technology

A hybrid active load and ideal synchronous condenser-based model for STATCOM applied to power flow studies

eISSN 2516-8401
Received on 18th March 2019
Revised 12th May 2019
Accepted on 29th May 2019
E-First on 31st July 2019
doi: 10.1049/iet-esi.2019.0031
www.ietdl.org

Ehsan Karami[1], Gevork B. Gharehpetian[1], Hassan Moradi CheshmehBeigi[2] ✉, Kumars Rouzbehi[3]

[1]*School of Electrical Engineering, Amirkabir University of Technology, Tehran, Iran*
[2]*Electrical Engineering Department, Faculty of Engineering, Razi University, Kermanshah 6714967346, Iran*
[3]*Department of Engineering, University of Seville, Seville, Spain*
✉ *E-mail: ha.moradi@razi.ac.ir*

Abstract: This study proposes a generalised STATCOM model employing active load and ideal synchronous condenser representation and its related power flow solution. The proposed method considers the effects of DC side voltage, internal switching losses, and operation mode on the power flow problem. To such aim, the proposed model tackles with a tap changing transformer accompanied by a variable conductance at the DC side in order to model the switching losses. This model can also take into account voltage regulation, reactive power control as well as amplitude modulation ratio and practical limitations. It is worth noting that the proposed model can be easily used for power flow studies by applying ordinary changes to the prevalent Newton–Raphson-based power flow methods. The introduced model is applied to two test systems including IEEE 14-Bus system, followed by a discussion on results.

Nomenclature

Constants

$E_{on}^{IGBT}, E_{off}^{IGBT}$	turn-on/off energy of IGBT
E_{off}^{D}	turn-off energy of diode due to reverse recovery charge current
U_0^{IGBT}, U_0^{D}	threshold voltage of IGBT/diode
f_{SW}	switching frequency
i_{ref}	on-state current of IGBT after commutation
V_{dc}	DC link voltage
V_{ref}	certain reference voltage for switching losses calculation (provided in data sheets)
Y_{ij}	nodal admittance matrix elements
R_{ij}, X_{ij}	leakage resistance/reactance of a transformer between buses i and j
R_{eq}	the equivalent resistance of both IGBT and diode
X_{eq}	equivalent reactance to model magnetic interface in VSC
ρ	a resultant resistant characteristic at rated voltage and current
ω	load current angular frequency
$\underline{I_i^{ST}}$	normal STATCOM terminal current at the bus i
$\underline{P_i^S}/\underline{Q_i^S}$	scheduled active/reactive power of bus i

Functions

P_L^{IGBT}, P_L^{D}	conduction losses of a single IGBT switch/diode
P_L^{VSC}	total conduction losses for a three-phase (six legs) VSC
P^{SW}	switching losses
P_{ij}, Q_{ij}	transferred active/reactive power between buses i and j
$\underline{P_i}, \underline{Q_i}$	active/reactive power of the bus i before installing STATCOM
P_i, Q_i	active/reactive power of the bus i after installing STATCOM
P_i^G, Q_i^G	generated active/reactive power of the bus i
$\Delta P_i, \Delta Q_i$	active/reactive power mismatch of the bus i

Variables

ϑ	amplitude modulation ratio
ψ	displacement angle between load current and fundamental component of the modulation function
$\overline{I_L}$	peak value of ac line current assumed to be sinusoidal
I_G^{SW}	required current at DC side to supply the switching losses
G^{SW}	current dependent conductance at DC side
I_i^{ST}	actual STATCOM terminal current at the bus i
V_i^{ST}	incoming voltage to STATCOM located at the bus i
δ_{ij}	phase shift between V_i and V_j
φ_i	phase angle of bus i

1 Introduction

High penetration of voltage sensitive devices in recent power systems has turned voltage consideration as an important issue of power system operators. It is usually caused by reactive power flow in both transmission and distribution systems. Hence, several attempts have been focused on reactive power flow control to provide an acceptable voltage profile [1]. Various reactive power compensators have been introduced and tested to this end [2].

Flexible Ac transmission system (FACTS) devices are modern static reactive compensators; they provide flexibility to power flow control which improves system performance. Such devices adjust generated/absorbed active/reactive power not only to control a set of specified parameters, but also to improve the damping of power system oscillations and active power loss reduction [3–7]. FACTS controllers are categorised as series and shunt compensators; the latter is devoted to provide voltage support at momentous buses of an electrical network. Static synchronous compensator (SVC) and its modern counterpart Static synchronous compensator (STATCOM) are the most popularly used shunt FACTS devices.

STATCOM is a voltage source converter (VSC)-based device, which increases the loadability margin [8]. It also independently provides active/reactive power generation/absorption while a kind of energy source is set on the DC side [9, 10]. To exchange the enjoined reactive power with the grid, PWM shifts the output current to lead or lag the terminal voltage tailored to the needs.

Due to widespread penetration of STATCOMs, several research works have been conducted to reveal its operational principles,

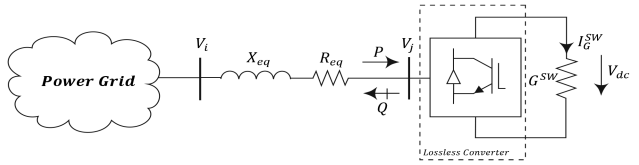

Fig. 1 *Conventional VSC along with the proposed lumped elements for IGBT losses*

model development including dynamic and static models, optimal power flow, and control strategies [11–21]. Among these, power flow study has been dedicated the most attention considering its importance in planning the future expansion of power systems as well as in determining the best operation of existing systems [14–20].

Prevalent STATCOM power flow models vary among PV and PQ bus representations proportional to the required application [16]. Besides these, voltage source-based model is another approach, which models STATCOM as a voltage source behind an equivalent impedance [10, 17]; it is also referred to power injection model in the specialised literature [18]. The main feature behind these models is in the ease of computer implementation; however, they exert several simplifications which confine to calculate switching losses, DC side voltage, and to apply different control strategies as well as the practical limitations. It is worth noting that in conventional PV and PQ node representation, STATCOM is usually assumed ideal and directly connected to the bus and then specified by its power flow parameters such as voltage and reactive power. However, for more accurate purposes, the internal impedance of STATCOM and power loss should be considered.

Various researches have been introduced to overcome the mentioned drawbacks. In [19], an equivalent voltage source model is proposed, in which dc voltage accompanied by the amplitude modulation ratio is used to find the STATCOM's AC voltage. Nevertheless, it should be modified to incorporate the switching losses as well as the load at the dc bus. In [20], basic operational characteristics of the FACTS controller for both phase and PWM control strategies are employed to justify the STATCOM stability model. Although different control strategies and operational limits are observed, power flow equations appear complicated. In [21], the effects of third harmonic injection on system power losses, submodule capacitance, circulating current, and fault current and mathematical models have been investigated.

In a recent contribution, [22] proposes a novel STATCOM model which is able to simultaneously describe basic principles of both AC and DC sides. It is based on the series connection of a VSC and its connecting transformer in which conductance is added in parallel at the DC side to model the switching losses. However, the method complicates the load flow equations which may cause difficulties while multiple STATCOMs are connected to the grid. Besides this, it does neither handle with reactive power control nor amplitude modulation ratio control.

As discussed, switching losses and detailed DC side representation are not often observed in STATCOM modelling of the aforementioned research. Moreover, simultaneous consideration of different control strategies, practical limitations, and facilitation of computer implementation are rarely referred up to now. This paper deals with new STATCOM modelling for power flow studies. First, prevalent switching and conduction losses in IGBT switches are accompanied by some simplifying assumptions to collaborate with load flow studies. As the most noteworthy contribution of this paper, a hybrid active load and ideal synchronous condenser representation are introduced for STATCOM applicable to the Newton–Raphson-based power flow methods. Moreover, a simple equivalent model is employed, which not only considers different control strategies and practical limitations but also facilitates ease of applying the STATCOM in computer implementation. Finally, the proposed method is developed in Matlab software environment and handled to two test systems, followed by presenting the results and comparing them to those of previous research.

2 IGBT losses

2.1 Switching and conduction losses in IGBT switches

STATCOM losses arise by switching losses and semiconductor conduction. While the former one varies depending on the semiconductors characteristics and switching frequency, the later gets affected by the VSC's output current [23]. As reported in [24], switching losses of a VSC equipped by IGBT switches in an AC network can be calculated by (1). In this equation, V_{ref} and i_{ref} represent certain reference voltage for switching losses calculation (provided in data sheets) and on-state current of IGBT after commutation, respectively

$$P^{\text{SW}} = \frac{6}{\pi} \cdot f_{\text{SW}} \cdot \left(E_{\text{on}}^{\text{IGBT}} + E_{\text{off}}^{\text{IGBT}} + E_{\text{off}}^{D}\right) \cdot \frac{V_{\text{dc}}}{V_{\text{ref}}} \frac{\overline{I_{\text{L}}}}{i_{\text{ref}}} \tag{1}$$

By increasing the temperature, load current, and dc voltage, the turn-on and turn-off losses in IGBT and diode power modules increase [25]. It is concluded from (1) that low dc voltage reduces switching losses.

The IGBT conduction losses are dependent on the employed modulation function; considering the commonly used sinusoidal pulse width modulation technique in which modulation function is assumed as $F_{\text{t}} = \vartheta \sin(\omega t)$, the conduction losses of a single IGBT switch and a diode are mentioned in (2), (3) [24]. Summation of (2) and (3) leads to total conduction losses which can be expressed for a three-phase (six legs) VSC by (4)

$$P_{\text{L}}^{\text{IGBT}} = U_0^{\text{IGBT}} \overline{I_{\text{L}}} \left(\frac{1}{2\pi} + \frac{\vartheta \cos\psi}{8}\right) + r_{\text{c}} \overline{I_{\text{L}}}^2 \left(\frac{1}{8} + \frac{\vartheta \cos\psi}{3\pi}\right) \tag{2}$$

$$P_{\text{L}}^{\text{D}} = U_0^{\text{D}} \overline{I_{\text{L}}} \left(\frac{1}{2\pi} - \frac{\vartheta \cos\psi}{8}\right) + r_{\text{D}} \overline{I_{\text{L}}}^2 \left(\frac{1}{8} - \frac{\vartheta \cos\psi}{3\pi}\right) \tag{3}$$

$$P_{\text{L}}^{\text{VSC}} = 6 \cdot \left(P_{\text{L}}^{\text{IGBT}} + P_{\text{L}}^{\text{D}}\right) \tag{4}$$

2.2 Simplifying assumptions

Some simplifying assumptions can be inserted to deal with IGBT losses in load flow studies. Fig. 1 shows the schematic diagram of a VSC. Assume that the dashed rectangle is lossless and the entire IGBT losses can be modelled in the lumped elements shown in Fig. 1. Considering such assumption, active power balance at the node j is as (5) since only active power flows through the converter. It can be concluded from this equation that $|I_{ij}|$ (AC side current flows from bus i to j) and I_{G}^{SW} are proportional as $|V_j|$ and V_{dc} are linked via modulation ratio

$$|V_j||I_{ij}| = V_{\text{dc}} I_{\text{G}}^{\text{SW}} \tag{5}$$

According to (1), $P^{\text{SW}} \propto V_{\text{dc}} \cdot \overline{I_{\text{L}}}$ in which $\overline{I_{\text{L}}}$ is peak value of I_{ij} and so it is also proportional to I_{dc}. Hence, an equivalent conductance (G^{SW}) can be defined at the DC side to model switching losses as

$$P^{\text{SW}} = V_{\text{dc}} I_{\text{G}}^{\text{SW}} = V_{\text{dc}} \left(G^{\text{SW}} V_{\text{dc}}\right) = G^{\text{SW}} V_{\text{dc}}^2 \tag{6}$$

where

$$G^{\text{SW}} = f\left(I_i^{\text{ST}}\right) + G_{\text{I}} \tag{7}$$

$$f\left(I_i^{\text{ST}}\right) = \rho \left(\frac{I_i^{\text{ST}}}{\underline{I_i^{\text{ST}}}}\right)^2 \tag{8}$$

The equivalent conductance represented in (7) consists of a current-dependent term accompanied by a constant value. The $f\left(I_i^{\text{ST}}\right)$ relates the switching losses to STATCOM's actual current and is calculated through (8) [22]. Besides this, G_{I} is used to

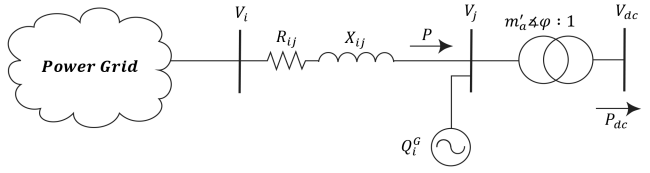

Fig. 2 *New VSC model*

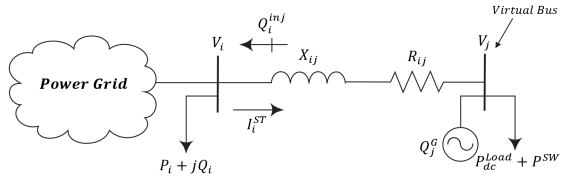

Fig. 3 *Proposed equivalent circuit of a STATCOM installed at the bus i of a power grid*

include losses when VSC operates isolated from the grid. In the case of neglecting switching losses, $G^{\mathrm{SW}} = 0$ and thus conventional STATCOM model is achieved.

As the second simplifying assumption, since the threshold voltages in IGBT and diode semiconductors are relatively small, the first terms of (2) and (3) can be neglected and so $P_{\mathrm{L}}^{\mathrm{VSC}} \propto \overline{I_{\mathrm{L}}}^2$. Hence, VSC conduction losses can be approximated to (9) in the linear region of operation. In this equation, I_{L} represents the RMS value of the AC side current and R_{eq} is equivalent resistance of both IGBT and diode which can also be added to the coupling transformer's series impedance

$$P_{\mathrm{L}}^{\mathrm{VSC}} = R_{\mathrm{eq}} I_{\mathrm{L}}^2 \tag{9}$$

3 Proposed STATCOM/VSC model and equivalent circuit for STATCOM/VSC

3.1 Proposed STATCOM/VSC model

The proposed STATCOM model consists of a tap changing transformer, ideal synchronous condenser, and coupling impedance. As current researches, the tap changing transformer shown in Fig. 2 represents the DC–AC connection of a VSC via (10). In this equation, the tap magnitude (m'_a) corresponds to the amplitude modulation ratio [22, 26]

$$V_j = m'_a \mathrm{e}^{\mathrm{j}\varphi} V_{\mathrm{dc}} \tag{10}$$

In general, DC side voltage is kept constant. Therefore, according to (10), AC side voltage is affected by DC side voltage and amplitude modulation ratio. Moreover, the reactive power of the VSC can be modelled by an external device. The absorbed active and generated reactive powers of the VSC (11), in which active power supplies DC side load, VSC's conduction, and switching losses

$$\begin{aligned} P &= \frac{V_j}{R_{ij}^2 + X_{ij}^2}\left[R_{ij}\left(V_i \cos\delta_{ij} - V_j\right) - X_{ij} V_i \sin\delta_{ij}\right] \\ Q &= -\frac{V_j}{R_{ij}^2 + X_{ij}^2}\left[R_{ij} V_i \sin\delta_{ij} + X_{ij}\left(V_i \cos\delta_{ij} - V_j\right)\right] \end{aligned} \tag{11}$$

Comparison between the exchanged reactive power shown in (8) and that of the ideal synchronous condenser reveals that an ideal synchronous condenser connected to the VSC terminal (bus j) can solely model the generated/absorbed reactive power of a VSC. By means of the proposed representation, current Newton–Raphson power flow equations remain unchanged in the presence of VSC as will be discussed in the next sections.

The coupling impedance in Fig. 2 represents both conduction losses and the magnetic interface. It should be noted that impedance values are selected based on descriptions reported on Section 2 as well as the information reported on data sheets.

3.2 Equivalent circuit for STATCOM model

The proposed STATCOM model consists of an internal virtual bus in which coupling impedance, tap changing transformer, and the ideal synchronous condenser are connected as shown in Fig. 3. To facilitate ease of computer implementation, an equivalent circuit is proposed in this figure which refers all DC side parameters to the AC side.

Since only active power flows through the ideal tap changing transformer (as discussed in Section 2), DC side loads in the secondary side can be transferred to the primary side. This is shown in Fig. 3 in which switching losses and DC side load are combined together and represented as an active load.

The proposed virtual bus voltage affects the required amplitude modulation ratio as expressed below

$$\frac{V_{\mathrm{dc}}}{1} = \frac{V_j}{m'_a \angle\varphi} \rightarrow V_j = (m'_a V_{\mathrm{dc}})\angle\varphi \tag{12}$$

$$m'_a = \frac{|V_j|}{V_{\mathrm{dc}}} \tag{13}$$

According to (12), the virtual bus angle is equal to φ which is directly obtained from load-flow studies. Besides this, tap magnitude is calculated by (13). It should be noted that m'_a changes according to VSC topology. For instance, for a two-level three-phase VSC, m'_a is $(\sqrt{3}/2)\vartheta$.

4 Power flow equations in presence of STATCOM

One of the main salient features of the proposed method is that no additional variable is required to form power-flow equations in the presence of SATCOM, except the internal virtual bus. As the virtual bus is solely connected to the bus i, it simply applies to the Jacobian matrix and can handle several operation modes. This section represents the power flow equations regarding STATCOM implementations. First, a general power flow equation is introduced in the presence of STATCOM and then different control strategies are applied to form the Jacobian matrix associated with each operation mode. According to power flow balance, active and reactive powers of the bus i before installing STATCOM are as follows [27]:

$$\begin{aligned} \underline{P_i} &= \sum_{k=2}^{n} |V_i||V_k||Y_{ik}|\cos(\delta_k - \delta_i + \theta_{ik}) \\ \underline{Q_i} &= -\sum_{k=2}^{n} |V_i||V_k||Y_{ik}|\sin(\delta_k - \delta_i + \theta_{ik}) \end{aligned} \tag{14}$$

The general form of Newton–Raphson power flow model in the presence of virtual bus can be represented as (15). In this case, both the active load and the ideal synchronous condenser connected to the virtual bus are added to power flow equations

$$\begin{bmatrix} \Delta P_i \\ \Delta Q_i \\ \Delta P_j \\ \Delta Q_j \end{bmatrix} = \begin{bmatrix} \frac{\partial P_i}{\partial \delta_i} & \frac{\partial P_j}{\partial \delta_j} & \frac{\partial P_i}{\partial |V_i|}|V_i| & \frac{\partial P_j}{\partial |V_j|}|V_j| \\ \frac{\partial Q_i}{\partial \delta_i} & \frac{\partial Q_j}{\partial \delta_i} & \frac{\partial Q_i}{\partial |V_i|}|V_i| & \frac{\partial Q_i}{\partial |V_j|}|V_j| \\ \frac{\partial P_j}{\partial \delta_i} & \frac{\partial P_j}{\partial \delta_j} & \frac{\partial P_j}{\partial |V_i|}|V_i| & \frac{\partial P_j}{\partial |V_j|}|V_j| \\ \frac{\partial Q_j}{\partial \delta_i} & \frac{\partial Q_j}{\partial \delta_j} & \frac{\partial Q_j}{\partial |V_i|}|V_i| & \frac{\partial Q_j}{\partial |V_j|}|V_j| \end{bmatrix} \begin{bmatrix} \Delta\delta_i \\ \Delta\delta_j \\ \frac{\Delta|V_i|}{|V_i|} \\ \frac{\Delta|V_j|}{|V_j|} \end{bmatrix} \tag{15}$$

It should be noted that the proposed model and solution method applies to fundamental power flow. However, by using switching functions, the model can be extended to consider harmonics injected to the grid and then the problem can be solved by using the harmonic domain.

4.1 Voltage control mode

In this mode of operation, STATCOM provides the required reactive power (Q_j^{G}) to retain the voltage magnitude of bus i (V_i) at the specified value. The partial derivation terms shown in (16) represent the Jacobian elements with respect to bus j variables while $Y_{jk} = 0$ for $k = 2, 3\ldots, n$ and $k \neq i, j$

$$\begin{aligned} &\frac{\partial P_k}{\partial \delta_j} = \frac{\partial P_k}{\partial |V_j|} = 0, \quad k = 2, 3, \ldots, n, \quad k \neq i, j \\ &\frac{\partial Q_k}{\partial \delta_j} = \frac{\partial Q_k}{\partial |V_j|} = 0, \quad k = 2, 3, \ldots, n, \quad k \neq i, j \end{aligned} \tag{16}$$

By eliminating the row associated to Q_j and the column related to V_i, the modified version of (14) and (15) under voltage control mode is achieved as (17) and (18), respectively. In comparison with (14), it can be seen that the proposed method has just led to changes in equations associated with active and reactive powers of the bus i

$$\begin{bmatrix} \Delta P_i \\ \Delta Q_i \\ \Delta P_j \end{bmatrix} = \begin{bmatrix} \frac{\partial P_i}{\partial \delta_i} & \frac{\partial P_j}{\partial \delta_j} & \frac{\partial P_j}{\partial |V_j|}|V_j| \\ \frac{\partial Q_i}{\partial \delta_i} & \frac{\partial Q_j}{\partial \delta_i} & \frac{\partial Q_i}{\partial |V_j|}|V_j| \\ \frac{\partial P_j}{\partial \delta_i} & \frac{\partial P_j}{\partial \delta_j} & \frac{\partial P_j}{\partial |V_j|}|V_j| \end{bmatrix} \begin{bmatrix} \Delta \delta_i \\ \Delta \delta_j \\ \frac{\Delta |V_j|}{|V_j|} \end{bmatrix} \tag{17}$$

$$\begin{aligned} P_i &= \underline{P_i} + |V_i||V_j||Y_{ij}|\cos(\delta_j - \delta_i + \theta_{ij}) \\ Q_i &= \underline{Q_i} - |V_i||V_j||Y_{ij}|\sin(\delta_j - \delta_i + \theta_{ij}) \end{aligned} \tag{18}$$

The required reactive power generated by the ideal synchronous condenser is

$$Q_j^{\mathrm{G}} = -|V_j|^2|Y_{ij}|\sin(\theta_{ij}) - |V_i||V_j||Y_{ij}|\sin(\delta_i - \delta_j + \theta_{ij}) \tag{19}$$

It should be noted that, if achieving a required level of reactive power is prohibited by limitations, Q_j^{G} is set to its maximum permissible value. Besides this, in some cases, a tap changing transformer might be used to provide the specified voltage level. The mismatch powers terms within each iteration (k) in case of voltage control mode are

$$\begin{aligned} \Delta P_i^{(k)} &= P_i^{\mathrm{S}} - P_i^{(k)} = \left(P_i^{\mathrm{G}} - P_i^{\mathrm{L}}\right) - P_i^{(k)} \\ \Delta Q_i^{(k)} &= Q_i^{\mathrm{S}} - Q_i^{(k)} = \left(Q_i^{\mathrm{G}} - Q_i^{\mathrm{L}}\right) - Q_i^{(k)} \\ \Delta P_j^{(k)} &= P_j^{\mathrm{S}} - P_j^{(k)} = \left(P_j^{\mathrm{G}} - P_j^{\mathrm{L}}\right) - P_j^{(k)}, P_j^{\mathrm{G}} = 0 \end{aligned} \tag{20}$$

Considering (20), it should be noted that if VSC is used, DC source which generates active power could be connected to the DC side. In this case, generated active power in the virtual bus is not equal to zero ($P_j^{\mathrm{G}} \neq 0$).

4.2 Reactive power control mode

While reactive power control mode is employed, Q_i^{inj} represented in Fig. 3 is set to a specified value; it shows the total reactive power injected to bus i and can be used for power factor correction. The Jacobian matrix of this mode is obtained by replacing Q_j by Q_i^{inj} in (15). Expanding (18) for buses shown in Fig. 3, the controlled reactive power is determined as follows:

$$Q_i^{\mathrm{inj}} = |V_i|^2|Y_{it}|\sin(\theta_{ij}) - |V_i||V_j||Y_{ij}|\sin(\delta_j - \delta_i + \theta_{ij}) \tag{21}$$

Mismatch power terms, in this case, are similar to that of voltage control mode except for $\Delta Q^{(k)}$ which should be considered as follows:

$$\Delta Q_i^{\mathrm{inj}(k)} = Q_i^{\mathrm{injS}} - Q_i^{\mathrm{inj}(k)} \tag{22}$$

4.3 Amplitude modulation control mode

In this mode of operation, the virtual bus acts as a PV bus and thus the row associated to Q_j and the column related to V_j are omitted from (15). The obtained Newton power flow model is as (23). It should be noted the mismatch power terms, in this case are similar to that of the voltage control mode

$$\begin{bmatrix} \Delta P_i \\ \Delta Q_i \\ \Delta P_j \end{bmatrix} = \begin{bmatrix} \frac{\partial P_i}{\partial \delta_i} & \frac{\partial P_j}{\partial \delta_j} & \frac{\partial P_j}{\partial |V_j|}|V_j| \\ \frac{\partial Q_i}{\partial \delta_i} & \frac{\partial Q_j}{\partial \delta_i} & \frac{\partial Q_i}{\partial |V_j|}|V_j| \\ \frac{\partial P_j}{\partial \delta_i} & \frac{\partial P_j}{\partial \delta_j} & \frac{\partial P_j}{\partial |V_j|}|V_j| \end{bmatrix} \begin{bmatrix} \Delta \delta_i \\ \Delta \delta_j \\ \frac{\Delta |V_i|}{|V_i|} \end{bmatrix} \tag{23}$$

4.4 Implementation aspects of the proposed method

4.4.1 State variables and increments: As mentioned before, there is no need for additional variables to describe the operation of STATCOM, except those of the virtual bus ($|V_j|$, δ_j). While increments of the state variables at iteration (k) associated with voltage and reactive power control modes are reported in (24), the amplitude modulation ratio control just deals with (25)

$$\begin{aligned} \Delta |V_j|^{(k)} &= |V_j|^{(k)} - |V_j|^{(k-1)} \\ \Delta \delta_j^{(k)} &= \delta_j^{(k)} - \delta_j^{(k-1)} \end{aligned} \tag{24}$$

$$\Delta \delta_j^{(k)} = \delta_j^{(k)} - \delta_j^{(k-1)} \tag{25}$$

4.4.2 Practical limits and power flow initialisation: There are some practical restrictions raised while STATCOM operates in an actual grid; the VSC is supposed to operate in the linear region, which should meet $0 < \vartheta < 1$ [28]. Moreover, considering the voltage and current limitations, minimum/maximum producible/absorbable reactive power of VSC must fall within an acceptable margin [3]. In addition, VSC overcurrent may cause thermal instability either in inductive or capacitive modes; this constraint may be applied to the VSC reactive power while its terminal voltage is supposed to be a constant value. Parameter initialisation of the proposed method is the same as conventional power flow. Initialisation of P^{SW} is carried out by (6) assuming $I_i^{\mathrm{ST}} = \underline{I_i^{\mathrm{ST}}}$ in (8).

5 Tests and results

In order to apply the proposed method for power flow solution in presence of STATCOM, it is implemented in Matlab software. To evaluate the effectiveness of the proposed method, the problem is solved for two test systems including a two-bus network and the IEEE 14-bus system [22, 29]. In all cases two-level, three-phase VSCs are employed. In these converters, equivalent amplitude modulation ratio is set equal to $\sqrt{3}/2 \cdot \vartheta$ [21].

5.1 First scenario test case I

In this test, a simple two-bus system shown in Fig. 4 is employed. It consists of a generator, a transmission line, and a VSC to maintain the second bus voltage at a specified value. While the generator node is assumed as Slack bus, the entire data are reported in [22]. In this system, $R_{12} = 0.05$, $X_{12} = 0.1$, $R_{\mathrm{TR}} = 0.05$, $X_{\mathrm{TR}} = 0.1$, $R_{\mathrm{VSC}} = 0.01$, $X_{\mathrm{VSC}} = 0.1$, $G_0 = 0.01$, and $B_{\mathrm{eq}} = 0.5$ all in p.u. The proposed method is conducted on this test system and the obtained load flow results are shown in Fig. 4. The simulation results reveal that the virtual bus voltage, shown in Fig. 3, is $1.133\angle -3.855°$ p.u. in which $-3.885°$ represents the phase shifter angle; considering (10), the required modulation ratio is 0.925. It has been found in the simulation that the VSC switching losses are 0.014 p.u., corresponding to $G^{\mathrm{SW}} = 0.7\%$ and the VSC line current is

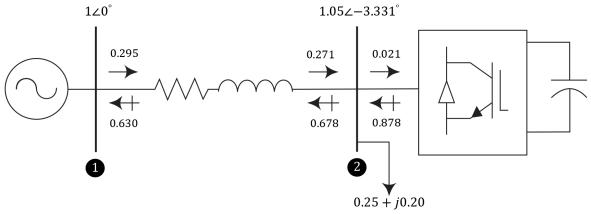

Fig. 4 *Simple two-bus system [22] and the obtained load flow results*

Table 1 Power flow results obtained by the proposed and conventional models

Quantity	Proposed model	Conventional model
bus 2 voltage, p.u.	1.050∠−3.331°	1.050∠−3.232°
virtual bus voltage, p.u.	1.133∠−3.855°	1.133∠−3.684°
amplitude modulation ratio	0.925	0.925
switching losses, p.u.	0.014	0.000
ohmic loss, p.u.	0.007	0.007
equivalent capacitive susceptance, p.u.	0.738	0.732
output reactive power, p.u.	0.878	0.870
VSC's terminal current, p.u.	0.837∠85.300°	0.829∠86.317°
# of iterations	7	7

Table 2 Comparison of different methods in the first scenario

Quantity	Operation mode					
	Voltage control mode $V_2 = 1.05\,\text{p.u.}$		Reactive power control mode $Q = 0.2\,\text{p.u.}$		Amplitude modulation ratio control mode $\vartheta = 0.85$	
	Proposed method	Refs. [22, 26]	Proposed method	Refs. [22, 26]	Proposed method	Refs. [22, 26]
bus 2 voltage, p.u.	1.050∠−3.374°	1.050∠−3.374°	0.986∠−1.572°	—	1.004∠−2.058°	—
virtual bus voltage, p.u.	1.134∠−3.928°	1.134∠−3.928°	1.006∠−1.805°	—	1.041∠−2.383°	—
amplitude modulation ratio	0.926	0.926	0.821	—	0.850	—
switching losses, p.u.	0.020	0.020	0.020	—	0.020	—
Ohmic loss, p.u.	0.007	0.007	4×10^{-4}	—	0.001	—
equivalent capacitive susceptance, p.u.	0.741	0.741	0.202	—	0.362	—
output reactive power, p.u.	0.882	0.882	0.200	—	0.378	—
VSC's terminal current, p.u.	0.840∠84.867°	0.840∠84.867°	0.204∠82.600°	—	0.377∠84.698°	—
# of iterations	7	7	7	—	6	—

0.837∠85.300° p.u. The algorithm converges in eight iterations to a tolerance of 10^{-8}; Table 1 summarises the load flow results for conventional STATCOM model. Comparing both models, it can be seen that switching losses affect the required active power produced by the generator and thus affect angles of voltage and current at bus 2. It should be noted that 'equivalent capacitive susceptance' shown in this table is defined by [22] which can provide the same amount of reactive power as that of the ideal synchronous condenser; in this paper, the equivalent capacitive susceptance is calculated by $B_{\text{eq},j} = (Q_j^{\text{G}}/|V_j|^2)$.

The same test system is also engaged to investigate the flexibility of the proposed solution method while considering other control modes. It is assumed that STATCOM modifies power factor of bus 2 by supplying 0.2 p.u. VAr under reactive power mode; ϑ is set to 0.85 subject to amplitude modulation ratio control mode. With the aim of comparison, the switching losses are assumed to be equal to 0.02 p.u. [22]. The procedure described in Section 4 is conducted and the obtained results are reported in Table 2. As seen in this table, both methods have achieved same solutions under voltage control mode. While the VSC's terminal current under amplitude modulation ratio control mode is 55% lesser than voltage control mode, ohmic losses are almost 85% decreased. The algorithm converges in seven and six iterations to a tolerance of 10^{-8} subject to reactive power control mode and amplitude modulation ratio control mode, respectively.

5.2 Test case II

In this scenario, the proposed approach is conducted on132 kV IEEE 14-bus transmission test system. It is assumed that a STATCOM is located at bus 14 (see Fig. 5) to overcome voltage collapse which is raised by reactive power demand [29]. While the entire electrical data in p.u. are assumed the same as [30], constant term of (7) is set to 0.0001 p.u. and the resultant resistant characteristic at rated voltage and current is supposed to be 0.01 p.u.; moreover, VSC and transformer impedances are lumped together and set equal to 0.01 + j0.1 p.u. [22].

The STATCOM is applied to network under different control modes; while in voltage control mode, STATCOM regulates V_{14} to 1.05 p.u., it injects 0.1 p.u. VAr to bus 14 under reactive power control mode. In amplitude modulation ratio control, ϑ is set to 0.8165 so that virtual bus voltage amplitude is set to 1 p.u. The obtained results of such examination are shown in Table 3 and Figs. 6 and 7. Table 3 illustrates the virtual bus voltage and output reactive power of STATCOM in different operation modes. While in reactive power control mode average voltage increases by 1.4%, this value decreases by 4.71% under amplitude modulation ratio control mode. The negative sign of output reactive power in amplitude modulation ratio expresses that STATCOM consumes reactive power in such a situation.

Figs. 6 and 7 represent voltage and angle profile of each mode, respectively. According to Fig. 6, STATCOM terminal voltage affects the voltage of neighbouring busses by affecting current flow

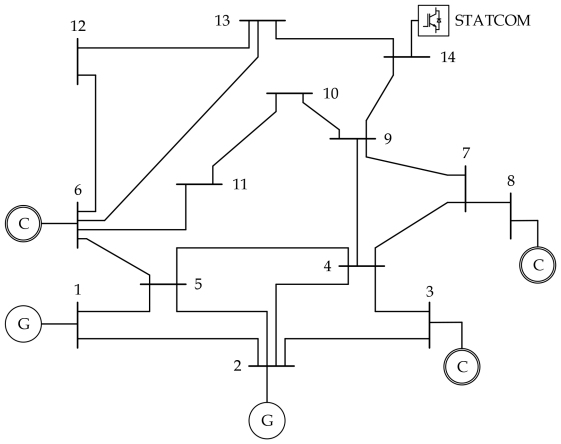

Fig. 5 *IEEE 14 bus test system along with STATCOM connected to bus 14*

Table 3 Virtual bus voltage and output reactive power in different operation modes

Operation mode	Virtual bus voltage, p.u.	Output reactive power, p.u.
voltage control	$1.057\angle -16.364°$	0.0724
reactive power control	$1.065\angle -16.501°$	0.1000
amplitude modulation control	$1.000\angle -18.348°$	−0.0655

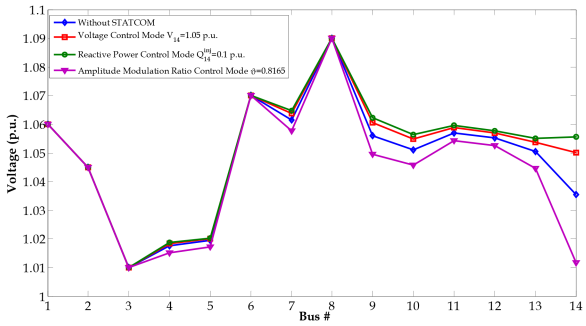

Fig. 6 *Voltage profile of the IEEE 14-bus system in different operation mode*

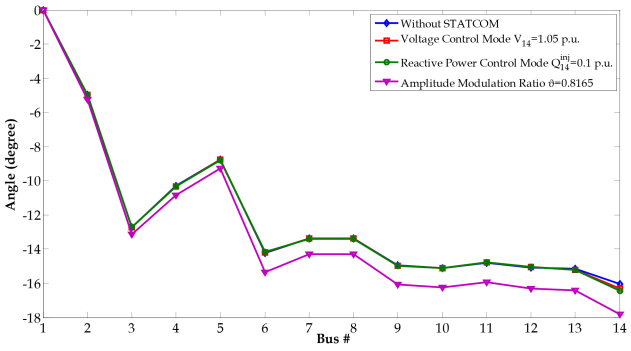

Fig. 7 *Angle profile of the IEEE 14-bus system in different operation mode*

through transmission lines. Differences in angle profiles in buses 2–13 in both voltage and reactive power control modes due to the increase in average voltage in comparison with the original network are small values. This difference at bus 14 is because of the active power loss of compensator. Selected value for ϑ affects both voltage profile and angle greatly; because in this case grid total loss due to increase in transmission line currents rises to 0.1528 p.u while these total power losses are 0.1332 and 0.1324 p.u. in compensated networks for $V_{14} = 1.05\,\text{p.u.}$ and $Q_{14}^{\text{inj}} = 0.1\,\text{p.u.}$, respectively.

In general, if DC side voltage is kept constant, by increasing amplitude modulation ratio, AC side voltage is also increased and

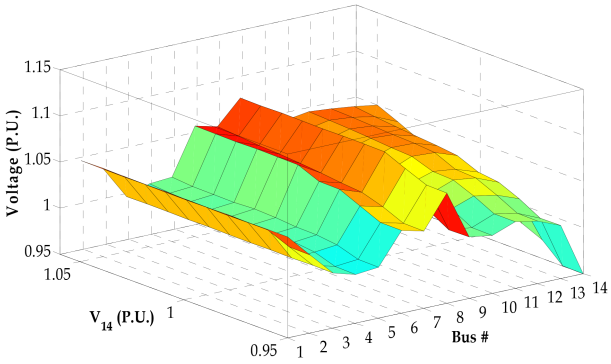

Fig. 8 *Voltage profile in voltage control mode*

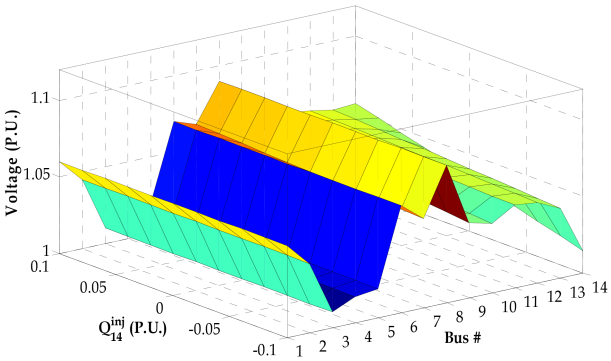

Fig. 9 *Voltage profile in reactive power control mode*

therefore, voltage profile is improved. In this case, angle profile also improves due to voltage profile improvement and therefore, there is a reduction in the current flow between different buses.

Different control strategies have been applied in a very wide range to study the effects of each mode. In voltage control mode, ideal synchronous condenser injects required reactive power to regulate V_{14} within the range of 0.95–1.05 p.u. In the range of 0.95 to 1.036 p.u., the direction of reactive power flow is from the grid to STATCOM and it consumes reactive power to achieve required voltage. However, in the range of 1.036–1.05 p.u., STATCOM generates reactive power to regulate terminal voltage. In reactive power control mode, Q_{14}^{inj} is varied from −0.1 to 0.1 p.u. For values within the bound −0.1 to 0 p.u. (relates to inductive mode), terminal voltage is less than its original value. However, for values from 0 to 0.1 p.u. (relates to capacitive mode) terminal voltage is more than its original value. Figs. 8 and 9 show voltage profile in voltage control mode and reactive power control mode, respectively. In each control mode, maximum number of iterations are seven to a tolerance of 10^{-8}. Due to voltage profile improvement, grid total loss decreases as the STATCOM's terminal voltage increases. Total active loss corresponding to $V_{14} = 0.95$ p.u. is 0.1513 and it is 0.1332 for $V_{14} = 1.05$ p.u. However, as explained in previous scenario STATCOM total active loss depend on terminal current. In reactive power control mode if Q_{14}^{inj} is set to 0.05 p.u., power factor of bus 14 is modified to one and V_{14} is $1.046\angle -16.235°$; in this case grid total active loss is 0.1334 p.u.

In order to evaluate the STATCOM's losses, power flow results for different terminal voltages are studied. Table 4 shows the total active loss for these instance voltages. As this table implies, by distancing from load flow results before installing STATCOM (original network), total active loss increases; because injected current increases and consequently related switching losses raise. This table also shows total STATCOM loss variations for $\rho = 0.05$ p.u.; by comparing the results, concludes that resultant resistant characteristic at rated voltage and current plays an important role in the amount of switching losses. As it is clear from Table 4, by changing V_{14} from 0.95 to 1.05 p.u. for $\rho = 0.01$ p.u. total STATCOM losses including conduction and switching losses vary from 1×10^{-6} to 0.0023 p.u. This variation for $\rho = 0.05$ p.u. is from 3×10^{-6} to 0.0084p.u. Fig. 9 depicts percent of STATCOM total

Table 4 Total STATCOM losses versus various terminal voltages

Features	ρ(p.u.)	V_{14}(p.u.)				
		0.950	0.980	1.000	1.036	1.050
total STATCOM loss, p.u.	0.01	0.0023	0.0015	0.0008	1×10^{-6}	1.5×10^{-4}
	0.05	0.0084	0.0050	0.0029	3×10^{-6}	0.0006
total active loss, p.u.	0.01	0.1513	0.1445	0.1410	0.1339	0.1332
	0.05	0.1584	0.1490	0.1429	0.1339	0.1346
per cent	0.01	1.5416	1.0367	0.5576	7.45×10^{-4}	0.1127
	0.05	5.3030	3.3557	2.0294	0.0022	0.4458

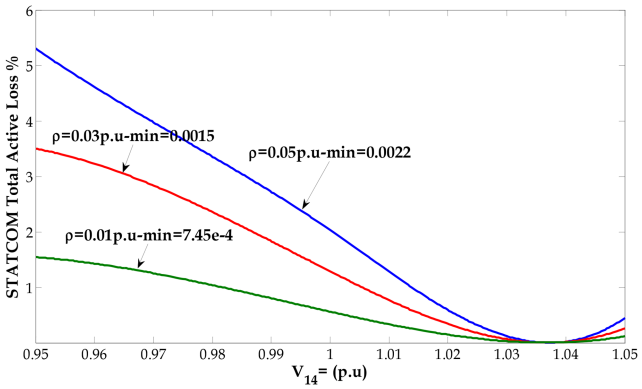

Fig. 10 *STATCOM total active loss versus different values of ρ*

active loss for different values of ρ. As expected, if V_{14} is set to 1.036 p.u. (bus 14 voltage in the original network) and constant term G_{I} in (7) is neglected, STATCOM terminal current is equal to zero; because no current flows from the STATCOM terminal and related G^{SW} and minimum value of STATCOM total active loss depicted in Fig. 10 are equal to zero. As discussed in Section 2 term G_{I} is used to incorporate the switching losses when STATCOM operates in floating or islanding mode. In this case, G_{I} is involved and switching losses should be supplied through the power grid.

6 Conclusion

A general VSC/STATCOM model has been proposed in this paper by appropriate modelling of switching losses for IGBT switches. Using active load and ideal synchronous condenser has been proposed to model switching losses and required reactive power, respectively. DC side load if exists is combined with switching losses as a constant term. This paper also described a comprehensive load flow solution for different STATCOM's operation modes based on Newton–Raphson load flow algorithm, which is capable of solving large and complex networks very effectively. Control strategies including voltage, output reactive power, and amplitude modulation ratio control modes along with their load flow solution have been discussed. The efficiency of both model and load flow solution (for different control strategies) have been illustrated by numeric examples and as the results show the proposed method can be used as a reliable algorithm for load flow studies in the presence of STATCOM.

7 References

[1] Miller, T.J.E.: '*Reactive power control in electric systems*' (Wiley Interscience, New York, 1982)

[2] Dixon, J., Moran, L., Rodriguez, J., *et al.*: 'Reactive power compensation technologies: state-of-the-art review', *Proc. IEEE*, 2005, **93**, (12), pp. 2144–2164

[3] Hingorani, G.N., Gyugyi, L.: '*Understanding FACTS: concepts and technologies of flexible AC transmission systems*' (IEEE, New York, 2000)

[4] Tadros, A., Khaldi, M.: 'STATCOM dynamic modeling and integration in power flow'. 3rd Int. Conf. on Advances in Computational Tools for Engineering Applications (ACTEA), Beirut, Lebanon, 2016, pp. 62–66

[5] Kumari, C.H.N., Sekhar, K.C.: 'Power flow control using FACTS device in modern power system'. 2017 IEEE Int. Conf. on Circuits and Systems (ICCS), Thiruvananthapuram, India, 2017

[6] Milano, F.: '*Power system modelling and scripting*' (Springer-Verlag, U.K., London, 2010)

[7] Fandi, G., Müller, Z., Straka, L., *et al.*: 'FACTS devices influence on power losses in transmission systems'. Proc. 2014 15th Int. Scientific Conf. on Electric Power Engineering (EPE), Brno, Czech Republic, 2014, pp. 29–33

[8] Sen, K.K.: 'Static synchronous compensator: theory, modeling and applications'. IEEE Power Engineering Society Winter Meeting, New York, NY, USA, 1999, vol. 2, pp. 1177–1183

[9] Lehn, P.W.: 'Exact modeling of the voltage source converter', *IEEE Trans. Power Deliv.*, 2002, **17**, (1), pp. 217–222

[10] Mathur, R.M., Varma, R.K.: '*Thyristor based facts controllers for electrical transmission systems*' (IEEE Press and Wiley Interscience, Piscataway, NJ, USA, 2002, 1st edn.)

[11] Edwards, C.W., Mattern, K.E., Stacey, E.J., *et al.*: 'Advance static VAR generator employing GTO thyristors', *IEEE Trans. Power Deliv.*, 1988, **3**, (4), pp. 1622–1627

[12] Petitclair, P., Bacha, S., Rognon, J.P., *et al.*: 'Averaged modeling and nonlinear control of an ASVC (advanced STATIC Var compensator)'. IEEE Power Electronics Specialists Conference, Baveno, Italy, 1996, pp. 753–758

[13] Pisey, A.D., Wagh, N.: 'Load flow analysis and incorporation of STATCOM to improve the voltage profile of Nagpur ring main system'. 2nd Int. Conf. on Trends in Electronics and Informatics (ICOEI), Tirunelveli, India, 2018, pp. 1–9

[14] Zaidi, A.H., Sunderland, K., Colon, M.: 'Role of reactive power (STATCOM) in the planning of distribution network with higher EV charging level', *IET Gener. Transm. Distrib.*, 2019, **13**, (7), pp. 951–959

[15] Kazemtabrizi, B., Acha, E.: 'An advanced STATCOM model for optimal power flows using Newton's method', *IEEE Trans. Power Syst.*, 2014, **29**, (2), pp. 514–525

[16] Acha, E., Fuerte-Esquivel, C.R., Ambriz-Perez, H., *et al.*: '*FACTS modeling and simulation in power networks*' (Wiley, New York, NY, USA, 2005)

[17] Wei, X., Chow, J.H., Fardanesh, B., *et al.*: 'A common modeling framework of voltage-sourced converters for load flow, sensitivity, and dispatch analysis', *IEEE Trans. Power Syst.*, 2004, **19**, (2), pp. 934–941

[18] Mosaad, M.I.: 'Model reference adaptive control of STATCOM for grid integration of wind energy systems', *IET Electr. Power Appl.*, 2018, **12**, (5), pp. 605–613

[19] Cañizares, C.A.: 'Power flow and transient stability models of FACTS controllers for voltage and angle stability studies'. IEEE Power Engineering Society Winter Meeting, Singapore, 2000, pp. 1447–1454

[20] Cañizares, C.A., Pozzi, M., Corsi, S., *et al.*: 'STATCOM modeling for voltage and angle stability studies', *Int. J. Electr. Power Energy Syst.*, 2003, **25**, pp. 431–441

[21] Li, R., Williams, B.W., Fletcher, J.E.: 'Influence of third harmonic injection on modular multilevel converter-based high-voltage direct current transmission systems', *IET Gener. Transm. Distrib.*, 2016, **10**, (11), pp. 2764–2770

[22] Acha, E., Kazemtabrizi, B.: 'A new STATCOM model for power flows using the Newton-Raphson method', *IEEE Trans. Power Syst.*, 2013, **28**, (3), pp. 2455–2465

[23] Casanellas, F.: 'Losses in PWM inverters using IGBTs', *IEE Proc., Electr. Power Appl.*, 1994, **141**, (5), pp. 235–239

[24] Bierhoff, M.H., Fuchs, F.W.: 'Semiconductor losses in voltage source and current source IGBT converters based on analytical derivation'. Proc. IEEE Power Electronics Specialists Conf., Aachen, Germany, 2004, pp. 2836–2842

[25] Blaabjerg, F., Pederson, J., Sigurjonsson, S., *et al.*: 'An extended model of power losses in hard-switched IGBT-inverters'. Proc. IEEE Industry Applications Conference, San Diego, CA, USA, 1996, pp. 1454–1463

[26] Tein, D.V.: 'Analysis and modelling of STATCOM for regulate the voltage in power systems'. 18th Int. Scientific Conf. on Electric Power Engineering (EPE), Kouty nad Desnou, Czech, 2017

[27] Glover, J.D., Mulukutla, S.: '*Power system analysis and design*' (PWS Publishing Company, Boston, 1994, 2nd edn.)

[28] Mohan, N., Undeland, T.M., Robins, W.P.: '*Power electronics: converters, applications and design*' (Wiley, New York, NY, USA, 2003)

[29] Lopes, B., Souza, A., Mendes, P.: 'Tangent vector as a tool for voltage collapse analysis considering a dynamic system model'. Power Tech ProG., Porto, Portugal, 2001, vol. 2, no. 5, pp. 1–6

[30] IEEE 14-Node Test System, available at: http://www.ee.washin-gton.edu/research/pstca